Generalized ray optics and orbital angular momentum carrying beams

2015 New J. Phys. 17 103034

(http://iopscience.iop.org/1367-2630/17/10/103034)

New Journal of Physics
The open access journal at the forefront of physics

Deutsche Physikalische Gesellschaft DPG
IOP Institute of Physics

Published in partnership with: Deutsche Physikalische Gesellschaft and the Institute of Physics

OPEN ACCESS

RECEIVED
9 June 2015

REVISED
26 August 2015

ACCEPTED FOR PUBLICATION
18 September 2015

PUBLISHED
16 October 2015

PAPER

Generalized ray optics and orbital angular momentum carrying beams

Václav Potoček[1,2] **and Stephen M Barnett**[1]

[1] School of Physics and Astronomy, University of Glasgow, University Avenue, Glasgow G12 8QQ, UK
[2] Czech Technical University in Prague, Faculty of Nuclear Sciences and Physical Engineering, Department of Physics, Břehová 7, 115 19 Praha 1, Czech Republic

E-mail: vaclav.potocek@glasgow.ac.uk

Keywords: ray optics, Wigner function, optical orbital angular momentum

Supplementary material for this article is available online

Abstract

In classical optics the Wolf function is the natural analogue of the quantum Wigner function and like the latter it may be negative in some regions. We discuss the implications this negativity has on the generalized ray interpretation of free-space paraxial wave evolution. Important examples include two classes of beams carrying optical orbital angular momentum—Laguerre–Gaussian (LG) and Bessel beams. We formulate their defining eigenfunction properties as phase–space symmetries of their Wolf functions, whose analytical form is shown, and discuss their interpretation in the ray picture. By moving to a more general picture of partly coherent fields, we find that new solutions displaying the same symmetries appear. In particular, we find that mixtures of Gaussian beams (thus fully describable using classical ray optics) can mimic the basic properties of LG beams without the need for negativity, and are not restricted to quantized values of angular momentum. The quantization of both the l and p parameters and negativity of the Wolf function are both inevitable and, indeed, arise naturally when a requirement on the purity of the solution is added. This work is supplemented by a set of computer animations, graphically illustrating the interpretative aspects of the described model.

Introduction

We know that most phenomena of light can only be explained when its wave nature is taken into account. Within the classical context, this has effectively eliminated attempts at a broader adoption of Newton's corpuscular description [1]. Nevertheless, geometric ray optics remains a good compromise between clarity and exactness in many real-world situations. Historically, its domain had been restricted to the limit of short wavelength, applicable to a good extent to many important fields including photography, microscopy, and telescopy, but failing at scales where interference phenomena can no longer be neglected.

The concept of generalized ray description of light waves, providing an exact mathematical model of light propagation and detection accounting even for interference phenomena, but keeping the intuitiveness of a geometric picture, dates back to the 1970's. First attempts can be identified in [2], after which the topic has been broadly—and to a good extent independently—developed by Bastiaans [3–5] and Sudarshan [6–8]. Simon [9] has noted that the ray picture becomes particularly plausible and well-behaved in the paraxial approximation, which was an ad hoc initial assumption in [2].

In order to successfully extend the ray picture of light to describe interference phenomena, some assumptions must be relaxed. Most notably, one must allow to consider rays carrying a negative intensity. These form the basis for describing destructive interference phenomena without the notion of a phase.

In this work, we apply the above ideas to the case of paraxial beams carrying optical orbital angular momentum (OAM) [10]. Laguerre–Gaussian (LG) beams, in particular, have been the target of a broad interest lately in connection to their use in, for example, optical tweezers and optical wrenches [11], multimode optical communication [12], or surface analysis [13], among many others, along with a recent development in the

accessibility of computer-generated holograms as a primary means of their fully customizable generation [14, 15]. Many important generalizations of practical applicability have been thoroughly studied, for example, beams with optical vortices displaced from their centroid [16]. The topic in turn is a part of a much broader field, extending also into the quantum optical domain where the spatial distributions are reflected in the sense of an abstract harmonic oscillator representation, allowing for methods similar to those described here to be employed [17, 18].

There certainly remains space for research in some of the theoretical aspects of OAM-carrying beams in their different representations. For example, a picture of a LG beam as formed by a sheaf of co-rotating rays had been repeatedly used in literature (see, for example, [19, 20], or in electron optics, [21]) inspired by the approximate shape of the integral curves of the Poynting vector [22, 23], only reaching this behaviour asymptotically for both azimuthal and radial indices simultaneously large [24]. This picture does not address the curvature of Poynting vector lines nor the divergence of its axial component near beam axis [25], the latter leading to a theoretical paradox [26]. By providing a complete generalized ray description of LG and Bessel beams, along with remarks on their interpretation, we aim to strengthen the methods currently in use as well as to resolve the aforementioned paradox and to provide new insights into the topic.

Paraxial wave equation and the Wolf function

Consider a weakly divergent monochromatic beam propagating along the $+z$ axis such that in its decomposition into plane waves, most of the intensity is concentrated in a close neighbourhood of $\vec{k} = (0,\, 0,\, k)$, $k = 2\pi/\lambda$. Let us ignore its polarization (or select one fixed polarization direction) and let the beam be described by a scalar function $\psi(x,\, y,\, z)$ obeying the Helmholtz equation

$$\left(\frac{\partial^2}{\partial x^2} + \frac{\partial^2}{\partial y^2} + \frac{\partial^2}{\partial z^2} + k^2\right)\psi(x,\, y,\, z) = 0. \tag{1}$$

Due to the paraxial structure of the beam, it can be assumed that most of the evolution along the z axis will be constituted by a linear phase ramp of $\mathrm{e}^{\mathrm{i}kz}$. Extracting this factor, let us define

$$u(x,\, y,\, z) \coloneqq \psi(x,\, y,\, z)\mathrm{e}^{-\mathrm{i}kz},$$

and represent the assumption of paraxiality by [27]

$$\left\|\frac{\partial^2}{\partial z^2}u(x,\, y,\, z)\right\| \ll k\left\|\frac{\partial}{\partial z}u(x,\, y,\, z)\right\| \tag{2}$$

in the L^∞ (supremal) norm.

On rewriting (1) in terms of $u(x,\, y,\, z)$ and applying neglections conforming to (2), we obtain the paraxial wave equation [27, 28, 30]:

$$\left(\frac{\partial^2}{\partial x^2} + \frac{\partial^2}{\partial y^2} + 2\mathrm{i}k\frac{\partial}{\partial z}\right)u(x,\, y,\, z) = 0. \tag{3}$$

In contrast with (1), this is a first-order evolution equation in z and thus only requires the specification of $u(x,\, y,\, z)$ at a single plane $z = z_0$ as the initial condition.

There is an exact formal agreement between the form of (3) and the $(2+1)$-dimensional free particle Schrödinger equation

$$\mathrm{i}\hbar\frac{\partial}{\partial t}\phi(x,\, y,\, t) = -\frac{\hbar}{2m}\left(\frac{\partial^2}{\partial x^2} + \frac{\partial^2}{\partial y^2}\right)\phi(x,\, y,\, t).$$

The agreement is complete if we identify the evolution parameter t with z and k with the Compton wave number $m/\hbar$ (both using $c = 1$).

Many quantum mechanical methods can then be directly translated into paraxial wave optical domain. One of the notable concepts is the Wigner function [29],

$$W_{\mathrm{qm}}\left(x,\, y,\, p_x,\, p_y \middle|\, t\right) = \frac{1}{\pi^2\hbar^2}\int \phi^*(x + x',\, y + y',\, t) \times \phi(x - x',\, y - y',\, t)\mathrm{e}^{2\mathrm{i}\left(x'p_x + y'p_y\right)/\hbar}\mathrm{d}x'\mathrm{d}y', \tag{4}$$

the analogue of which, in wave optics, is the Wolf function [6]

$$W\left(x,\, y,\, k_x,\, k_y\middle|z\right) = \frac{1}{\pi^2}\int u^*(x+x',\, y+y',\, z) \times u(x-x',\, y-y',\, z)\mathrm{e}^{2\mathrm{i}\left(x'k_x+y'k_y\right)}\mathrm{d}x'\mathrm{d}y'. \tag{5}$$

In the following, we shall assume both functions to be normalized in the L^1 norm (although it is more natural for the latter to integrate to the full cross-sectional intensity). This is automatically satisfied if $\phi(x,\, y,\, t)$ or $u(x,\, y,\, z)$ are L^2-normalized, respectively. Further, we shall drop the reference to the evolution parameter z in $W(x,\, y,\, k_x,\, k_y|z)$ where its value has been fixed and no ambiguity can occur.

Equations (4) or (5) assign a real-valued phase–space function to any given wave function $\phi(x,\, y,\, t)$ or a paraxial beam cross section $u(x,\, y,\, z)$, respectively. In many respects these functions can be interpreted as a probability (in the case of W_{qm}) or intensity (for W) distribution in a restricted sense. Notably,

$$\int W\left(x,\, y,\, k_x,\, k_y\middle|z\right)\mathrm{d}k_x\mathrm{d}k_y = |u(x,\, y,\, z)|^2,$$
$$\int W\left(x,\, y,\, k_x,\, k_y\middle|z\right)\mathrm{d}x\mathrm{d}y = \left|\tilde{u}\left(k_x,\, k_y,\, z\right)\right|^2, \tag{6}$$

where $\tilde{u}$ denotes the two-dimensional Fourier transform of the wave function u, among many other properties.

Of particular interest in phase–space formulation of quantum mechanics is that expectation values of observables can be computed averaging their phase–space representations using W_{qm} as the weight. This representation, called the (Weyl's) symbol f_A of an operator $\hat{A}$, is in this case obtained by

$$f_A\left(x,\, y,\, p_x,\, p_y\right) = \int \left\langle x-\frac{x'}{2},\, y-\frac{y'}{2}\middle|\hat{A}\middle|x+\frac{x'}{2},\, y+\frac{y'}{2}\right\rangle \times \mathrm{e}^{\mathrm{i}\left(x'p_x+y'p_y\right)/\hbar}\mathrm{d}x'\mathrm{d}y'.$$

Note in particular that W_{qm} is, up to a prefactor of $(2\pi\hbar)^{-2}$, the symbol of the density matrix of the state. A similar theorem holds also for the Wolf function with obvious interpretational differences, primarily expectation values becoming ensemble averages. The mapping of the two formalisms is achieved by replacing $\hbar$ by unity, time by the z coordinate, and components of momentum by those of wave vector perpendicular to the direction of propagation. In this respect, we will also speak of density operator $\rho(z)$ corresponding to a wavefront $u(x,\, y,\, z)$

$$\langle x,\, y|\,\rho(z)|x',\, y'\rangle = u(x,\, y,\, z)u^*(x',\, y',\, z), = \psi(x,\, y,\, z)\psi^*(x',\, y',\, z), \tag{7}$$

representing the equal-time second-order cross-correlation function of the monochromatic field [30], and we will carry the notation of a symbol of an operator to paraxial optical systems.

The evolution equation (3) can be rewritten for the Wolf function as follows:

$$\frac{\partial}{\partial z}W = -\frac{1}{k}\left(k_x\frac{\partial}{\partial x}+k_y\frac{\partial}{\partial y}\right)W, \tag{8}$$

and explicitly solved as

$$W\left(x,\, y,\, k_x,\, k_y\middle|z+\Delta z\right) = W\left(x-\frac{k_x}{k}\Delta z,\, y-\frac{k_y}{k}\Delta z,\, k_x,\, k_y\middle|z\right). \tag{9}$$

This result can be interpreted in a direct correspondence to the phase–space intensity density picture: the local density is preserved along straight trajectories of the slope $(k_x,\, k_y,\, k)$ in the $(x,\, y,\, z)$ space, keeping k_x and k_y constant. Thus, in terms of measurable physical quantities, any solution to the paraxial wave equation (3) can be decomposed into a set of ideal, non-interacting, linear rays going through every point of the cross section in every direction and carrying a positive, zero, or negative contribution to local intensity.

The possibility of negative values is an inherent property of the Wolf function and the only solutions of (3) with a completely non-negative Wolf function are Gaussian beams [31]. It is important to emphasize at this point that negative rays can never be directly observed. This is precluded by marginalization (6) in position or transverse k detection, which always yields non-negative values, or in general by the positivity of measurement operators when more intricate measurements are performed. In an intuitive understanding, positive rays are always stronger in total intensity in any phase–space cell of $\Delta x\Delta k_x \gtrsim 1$, $\Delta y\Delta k_y \gtrsim 1$ than negative ones and trying to separate the latter would inevitably overcome the diffraction limit, compromising the validity of the equations and approximations used.

LG beams

A LG mode is a prototypical example of an optical beam carrying OAM. Its form is stable under free-space propagation (only the scale of the intensity profile in a cross section changes) and each photon carries a constant integer number of OAM quanta, $L = l\hbar$. Here and in the following, unless explicitly stated otherwise, we shall always assume that coordinates are chosen such that z coincides with the beam axis and $z = 0$ is the point of the narrowest cross section, the beam waist. An LG beam is then completely specified by $l \in \mathbb{Z}$, an integer 'radial' parameter $p \geqslant 0$, and the width at the waist w_0, and often denoted $\mathrm{LG}_{l,p}$. The mathematical form of its wavefront in the scalar theory is [10]

$$u(r,\,\phi,\,z) \propto \frac{1}{w(z)}\left(\frac{r}{w(z)}\right)^{|l|} \mathrm{e}^{-\frac{r^2}{2w^2(z)}} \times L_p^{|l|}\left(\frac{r^2}{w^2(z)}\right) \mathrm{e}^{\mathrm{i}k\frac{r^2}{2R(z)}} \mathrm{e}^{\mathrm{i}l\phi} \mathrm{e}^{-\mathrm{i}(2p+|l|+1)\zeta(z)}.$$

Here,

$$w(z) = w_0\sqrt{1+\left(\frac{z}{z_\mathrm{R}}\right)^2}$$

denotes the beam width at z, reducing to the beam waist[3] w_0 at $z = 0$,

$$R(z) = z\left(1+\left(\frac{z_\mathrm{R}}{z}\right)^2\right)$$

the radius of curvature, and

$$\zeta(z) = \arctan\frac{z}{z_\mathrm{R}}$$

the Gouy phase. In all the above formulae,

$$z_\mathrm{R} = kw_0^2$$

is the Rayleigh range of the beam.

The mathematical form of the beam is the simplest in the beam waist, where

$$u(r,\,\phi,\,0) \propto r^{|l|}\mathrm{e}^{-\frac{r^2}{2w_0^2}} L_p^{|l|}\left(\frac{r^2}{w_0^2}\right)\mathrm{e}^{\mathrm{i}l\phi}. \tag{10}$$

This function can be found as a joint eigenfunction of the differential angular momentum operator

$$\hat{L} = -\mathrm{i}\left(x\frac{\partial}{\partial y} - y\frac{\partial}{\partial x}\right) \tag{11}$$

and an 'energy' operator

$$\hat{E} = \frac{1}{2w_0^2}\left(x^2+y^2\right) + \frac{w_0^2}{2}\left(\left(-\mathrm{i}\frac{\partial}{\partial x}\right)^2 + \left(-\mathrm{i}\frac{\partial}{\partial y}\right)^2\right), \tag{12}$$

corresponding to eigenvalues l and $2p + |l| + 1$, respectively.

As both operators are quadratic in position and momenta observables, their respective eigenvector equations correspond to phase–space symmetries of the Wolf functions of the LG beams: in general, for any operator $\hat{A}$ satisfying this condition, the Wolf function of the commutator $\hat{A}\rho - \rho\hat{A}$ corresponds, up to a constant factor, to the Poisson bracket of the Wolf function assigned to ρ and the symbol of the operator $\hat{A}$. For $u(x,\,y,\,z)$ satisfying the eigenvector equation

$$\hat{A}\,u(x,\,y,\,z) = \lambda u(x,\,y,\,z),$$

the density operator (7) commutes with $\hat{A}$, and therefore the Wolf function (5) satisfies

$$\left\{f_A,\,W\right\} = \frac{\partial f_A}{\partial x}\frac{\partial W}{\partial k_x} + \frac{\partial f_A}{\partial y}\frac{\partial W}{\partial k_y} - \frac{\partial f_A}{\partial k_x}\frac{\partial W}{\partial x} - \frac{\partial f_A}{\partial k_y}\frac{\partial W}{\partial y} = 0.$$

The symbols of operators (11) and (12) are

$$f_L\left(x,\,y,\,k_x,\,k_y\right) = xk_y - yk_x =: \lambda \tag{13}$$

[3] Corresponding here to an intensity drop by a factor of $1/e$ in the Gaussian case $l = p = 0$. The more usual $1/e^2$ half-width w_0' is related by $w_0' = \sqrt{2}\,w_0$.

and

$$f_E\left(x, y, k_x, k_y\right) = \frac{1}{2w_0^2}\left(x^2 + y^2\right) + \frac{w_0^2}{2}\left(k_x^2 + k_y^2\right) =: \epsilon,$$

leading to a rotational symmetry of the Wolf function of any LG beam with respect to

$$\begin{aligned} x &\mapsto x\cos\alpha - y\sin\alpha, \\ y &\mapsto y\cos\alpha + x\sin\alpha, \\ k_x &\mapsto k_x\cos\alpha - k_y\sin\alpha, \\ k_y &\mapsto k_y\cos\alpha + k_x\sin\alpha, \end{aligned} \tag{14}$$

and a symmetry with respect to the fractional phase–space Fourier transform,

$$\begin{aligned} x &\mapsto x\cos\beta + w_0^2 k_x\sin\beta, \\ y &\mapsto y\cos\beta + w_0^2 k_y\sin\beta, \\ k_x &\mapsto k_x\cos\beta - w_0^{-2}x\sin\beta, \\ k_y &\mapsto k_y\cos\beta - w_0^{-2}y\sin\beta, \end{aligned} \tag{15}$$

respectively.

The Wolf function of a LG beam in the beam waist can be computed using further properties of these symmetries, as demonstrated very elegantly by Simon and Agarwal in [32], or using a set of ladder operators for the l and p numbers, an approach taken by Vanvalkenburgh [33]. The result can be written in a compact form, manifestly symmetric with respect to (14) and (15),

$$W\left(x, y, k_x, k_y\right) = \frac{(-1)^{u+v}}{\pi^2}\mathrm{e}^{-(\mu+\nu)}L_u(2\mu)L_v(2\nu) =: \tilde{W}(\mu, \nu), \tag{16}$$

where

$$\begin{aligned} \mu &= \frac{1}{2}\left(w_0^{-1}x + w_0 k_y\right)^2 + \frac{1}{2}\left(w_0^{-1}y - w_0 k_x\right)^2 = \epsilon + \lambda, \\ \nu &= \frac{1}{2}\left(w_0^{-1}x - w_0 k_y\right)^2 + \frac{1}{2}\left(w_0^{-1}y + w_0 k_x\right)^2 = \epsilon - \lambda, \end{aligned} \tag{17}$$

and

$$(u, v) = \begin{cases} (p + l, p), & \text{if } l \geqslant 0, \\ (p, p - l), & \text{otherwise.} \end{cases}$$

The coordinates μ and ν, which both range from zero to infinity, can be supplemented by two angular coordinates $\phi_1, \phi_2 \in (0, 2\pi)$ to parametrize the full phase–space:

$$\left\{\begin{aligned} x &= \frac{w_0}{2}\left(x_+ + x_-\right), \\ y &= \frac{w_0}{2}\left(y_+ + y_-\right), \\ k_x &= \frac{1}{2w_0}\left(y_+ - y_-\right), \\ k_y &= \frac{1}{2w_0}\left(x_+ - x_-\right), \end{aligned}\right\}, \qquad \left\{\begin{aligned} x_+ &= \sqrt{2\mu}\cos\phi_1, \\ y_- &= \sqrt{2\mu}\sin\phi_1, \\ x_- &= -\sqrt{2\nu}\cos\phi_2, \\ y_+ &= -\sqrt{2\nu}\sin\phi_2, \end{aligned}\right\}. \tag{18}$$

Indeed, the conditions on constant μ and ν, or constant ϵ and λ, define a torus in the phase–space, which can then be parametrized by ϕ_1 and ϕ_2. The Jacobian of the coordinate transform $|\partial(x, y, k_x, k_y)/\partial(\mu, \nu, \phi_1, \phi_2)|$ is a constant $1/4$. Note that the symmetry transform (14) corresponds to displacing both ϕ_1 and ϕ_2 simultaneously by α while (15) corresponds to displacing (ϕ_1, ϕ_2) to $(\phi_1 + \beta, \phi_2 - \beta)$.

From (16) and the definitions (17) we deduce that rays too strong in either displacement or angle are superexponentially suppressed. As mentioned earlier, the case $l = p = 0$ (Gaussian beam) is the only Wolf function that is completely positive. As soon as u or v are non-zero, there will be a sign change when μ or ν cross each root of the corresponding Laguerre polynomial. An example of the Wolf function of LG_{11} is shown in figure 1. A typical cross section in the ray decomposition provided by interpreting the Wolf function as a generalized phase–space intensity is illustrated in figure 2.

The graphic representation displays several features of the Wolf function when interpreted as a phase–space intensity density. As expected, a majority of the total positive intensity lies in the half-plane corresponding to the sign of the λ coordinate matching that of l (rays co-rotating with the beam), but the separation is not exclusive. Also, one can clearly see that the function is regular and bounded over its entire domain. This is contrary to the

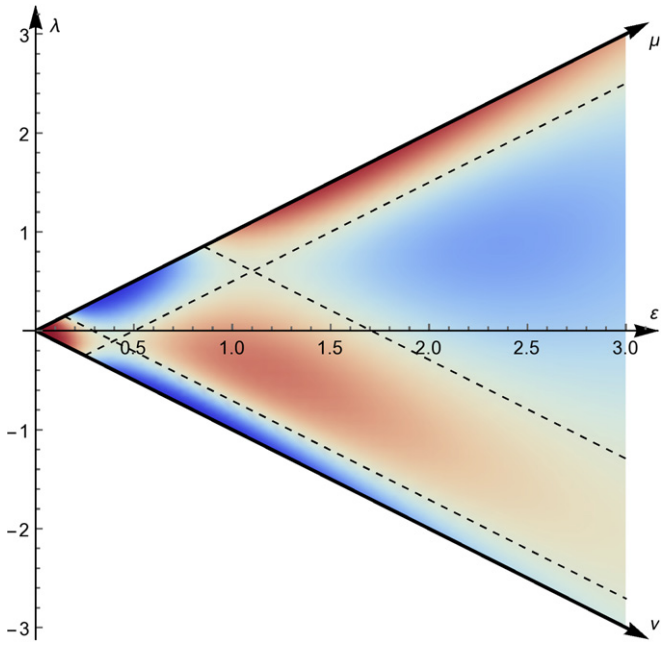

Figure 1. The Wolf function of a Laguerre–Gaussian beam LG_{11} in terms of μ and ν coordinates. Every pixel represents a value constant over the surface of a torus parametrized by the coordinates $\phi_{1,2}$. Blue shades represent positive and red shades negative values, nodal lines (gray) are dashed. The color function scaling is arbitrary.

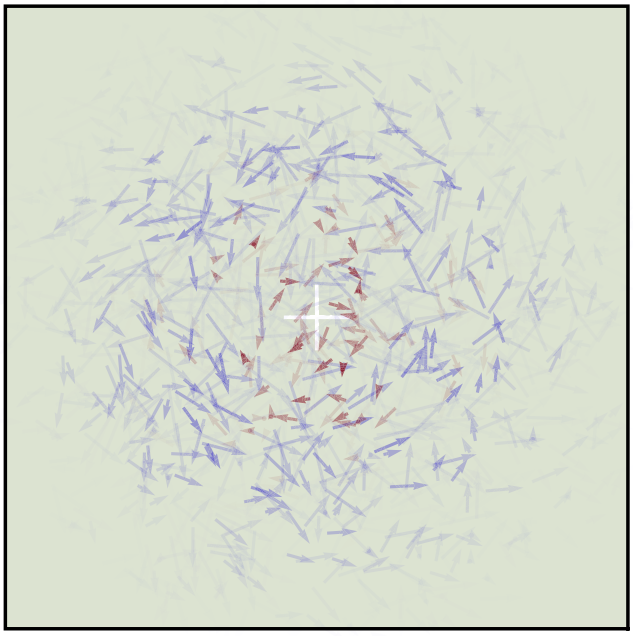

Figure 2. The cross section of a Laguerre–Gaussian beam LG_{10} at beam waist. Individual arrows represent samples from the phase–space distribution given by the Wolf function (16). The position and direction are proportional to (x,y) and $(k_x,\ k_y)$ coordinates, respectively. Blue shades represent positive and red shades negative values of the Wolf function, with opacity proportional to its value (a nonlinear correction has been applied to make the features better pronounced). 5000 random samples were taken from an uniform distribution over the interval of $(-2w_0,\ 2w_0)$ in each spatial coordinate (corresponding to the area covered by the plot) and $(-2w_0^{-1},\ 2w_0^{-1})$ in each momentum coordinate.

behaviour of Poynting vector near the origin, leading to a famous problem of anomalous momentum kick discrepancy [26]. This problem has been solved by an exact treatment of a test particle's uncertainty relation but the generalized ray picture shows that its very occurence can be attributed to the limitation to Euclidean space. The problem is not observed when full phase–space is considered.

The separate occurrences of the μ and ν coordinates in (16) make it easy to integrate to obtain the mean values

$$\begin{aligned}\langle\mu\rangle &:= \int_{\mathbb{R}^4} \mu W\left(x, y, k_x, k_y\right)\mathrm{d}x\mathrm{d}y\mathrm{d}k_x\mathrm{d}k_y,\\ &= \frac{1}{4}\int_0^\infty \mathrm{d}\mu \int_0^\infty \mathrm{d}\nu \int_0^{2\pi} \mathrm{d}\phi_1 \int_0^{2\pi} \mathrm{d}\phi_2\ \mu\tilde{W}(\mu, \nu) = 2u + 1\end{aligned}$$

and similarly

$$\langle\nu\rangle := \int_{\mathbb{R}^4} \nu W\left(x, y, k_x, k_y\right)\mathrm{d}x\mathrm{d}y\mathrm{d}k_x\mathrm{d}k_y = 2v + 1.$$

It follows that the weighted average of $\lambda = (\mu - \nu)/2$ and $\epsilon = (\mu + \nu)/2$ are $u - v = l$ and $u + v + 1 = 2p + |l| + 1$, matching the respective eigenvalues in the wavefunction picture. This example, albeit being a simple demonstration of the more general theorem mentioned above, underlines the plausibility but also practicality of treating the Wolf function (16) as a phase-space quasi-density of intensity.

The Supplementary Material to this work presents several cases of LG beams as computer animations of figure 2 in evolution along the z-axis.

Bessel beams

Bessel beams are rotationally symmetric, non-diffusive solutions to the Helmholtz equation (1)

$$\psi(r, \phi, z) \propto J_l(\kappa r)\mathrm{e}^{\mathrm{i}l\phi}\mathrm{e}^{\mathrm{i}k_z z},$$

where $l \in \mathbb{Z}$ and $k^2 = \kappa^2 + k_z^2$. The reduced function

$$u(r, \phi, z) \propto J_l(\kappa r)\mathrm{e}^{\mathrm{i}l\phi}\mathrm{e}^{\mathrm{i}\left(k_z - k\right)z} \tag{19}$$

is also a solution to the paraxial wave equation (3) but with $k_z = k - \kappa^2/(2k)$ instead of $\sqrt{k^2 - \kappa^2}$.

Like the LG beams, they satisfy

$$\hat{L}u(x, y, z) = -\mathrm{i}\frac{\partial}{\partial\phi}u(r, \phi, z) = lu(r, \phi, z). \tag{20}$$

The eigenvalue property of (12) is replaced by

$$\left(\left(-\mathrm{i}\frac{\partial}{\partial x}\right)^2 + \left(-\mathrm{i}\frac{\partial}{\partial y}\right)^2\right)u(x, y, z) = \kappa^2 u(r, \phi, z), \tag{21}$$

which grants the stability of the solution with respect to (3).

Bessel beams are non-normalizable as a beam with a wavefront of the form (19) with any non-zero amplitude would carry an infinite amount of energy. The Wolf function can still be introduced but some of its properties will be modified in connection to its own unnormalizability. In order to compute it, we rewrite $u(r, \phi, 0)$ as a generalized superposition of two-dimensional plane waves:

$$J_l(\kappa r)\mathrm{e}^{\mathrm{i}l\phi} = \frac{1}{2\pi}\int_0^{2\pi} \mathrm{e}^{-\mathrm{i}l\chi}\mathrm{e}^{\mathrm{i}x\kappa\,\sin\,\chi + \mathrm{i}y\kappa\,\cos\,\chi}\mathrm{d}\chi.$$

From here it only takes a direct application of (5) to reach the Wolf function

$$\begin{aligned}&W(x, y, \kappa\,\cos\,\alpha\,\cos\,\beta, \kappa\,\cos\,\alpha\,\sin\,\beta)\\ &= \frac{1}{2\pi^2\kappa^2\,\sin\,\alpha\,\cos\,\alpha}\,\cos(2\kappa x\,\sin\,\alpha\,\sin\,\beta - 2\kappa y\,\sin\,\alpha\,\cos\,\beta - 2\,l\alpha).\end{aligned} \tag{22}$$

Note that the latter two arguments of the left-hand side are expressed indirectly and only values for which $k_x^2 + k_y^2 \leqslant \kappa^2$ are reachable. For all other phase–space points the value is zero. The assignment of α and β to a given k_x and k_y within the supporting domain is not unique but any choice leads to the same value of the right-hand side of (22).

Bessel beams do not feature a naturally defined beam width so they do not have a particularly simple form in the coordinates $(\mu, \nu, \phi_1, \phi_2)$, defined above, for any w_0. They can be thought of as having an infinite value thereof, and thus an infinite Rayleigh range, in agreement with their zero diffraction. This is further supported by the fact that a Bessel beam can be obtained as a limit of LG beams as $p \to \infty$ and $w_0 = 2\sqrt{p}/\kappa$ [34, equation (22.15.2)], as also noted in [24]; also the eigenvalue equation

$$\hat{E}u = (2p + |l| + 1)u$$

becomes (21) under the same limiting conditions. Bessel beams are symmetric with respect to canonical transforms generated by angular momentum (13) and by

$$f_H\left(x,\, y,\, k_x,\, k_y\right) = k_x^2 + k_y^2 =: \eta,$$

which is the symbol of the differential operator on the left-hand side of (21), conveniently denoted $\hat{H}$ [4].

The value η, interpreted as a coordinate in phase–space, can be thought of as twice the limit of the above introduced ϵ in the infinite beam waist limit, rescaled by an appropriate power of w_0:

$$\eta = \lim_{w_0\to\infty} \frac{2\epsilon}{w_0^2} = \lim_{w_0\to\infty} \frac{\mu+\nu}{w_0^2}. \tag{23}$$

The coordinate $\lambda = (\mu - \nu)/2$ is still natural to the system due to (20). We perform an analogous transform on the angular coordinates, replacing them by their average

$$\theta := \lim_{w_0\to\infty} \frac{\phi_1+\phi_2}{2} = \arg\left(k_y - \mathrm{i}k_x\right)$$

and a renormalized limit of half of their difference,

$$\chi := \lim_{w_0\to\infty} w_0^2 \frac{\phi_1-\phi_2}{2} = \frac{k_x x + k_y y}{k_x^2+k_y^2}. \tag{24}$$

Clearly the Jacobian of the transform

$$\left| \frac{\partial\left(\frac{\mu+\nu}{w_0^2}, \frac{\mu-\nu}{2}, \frac{\phi_1+\phi_2}{2}, w_0^2\frac{\phi_1-\phi_2}{2}\right)}{\partial\left(\mu,\, \nu,\, \phi_1,\, \phi_2\right)} \right| = \frac{1}{2}$$

for all w_0 and thus also $|\partial(x,\, y,\, k_x,\, k_y)/\partial(\eta,\, \lambda,\, \theta,\, \chi)| = 1/2$. The Cartesian phase–space coordinates can be expressed using the new four-tuple as

$$\begin{aligned} x &= \frac{\lambda}{\sqrt{\eta}} \cos\theta - \chi\sqrt{\eta}\, \sin\theta, \\ y &= \frac{\lambda}{\sqrt{\eta}} \sin\theta + \chi\sqrt{\eta}\, \cos\theta, \\ k_x &= -\sqrt{\eta}\, \sin\theta, \\ k_y &= \sqrt{\eta}\, \cos\theta. \end{aligned}$$

In the new coordinates the Wolf function (22) is expressible solely in terms of η and λ as

$$W(\eta,\, \lambda,\, \theta,\, \chi) = \begin{cases} \dfrac{1}{2\pi^2\sqrt{\eta\left(\kappa^2-\eta\right)}} \cos\left(2\sqrt{\dfrac{\kappa^2-\eta}{\eta}}\,\lambda - 2\,l\, \arccos\dfrac{\sqrt{\eta}}{\kappa}\right) & \text{for } \eta < \kappa^2, \\ 0 & \text{otherwise} \end{cases} \tag{25}$$

(for a graph, see figure 3) and thus exhibits a symmetry with respect to translations in both θ and χ. The former is the same rotational symmetry as in (14). The latter generates the transform group

$$\begin{aligned} x &\mapsto x + \zeta k_x, \\ y &\mapsto y + \zeta k_y, \\ k_x &\mapsto k_x, \\ k_y &\mapsto k_y, \end{aligned} \tag{26}$$

as $\chi \mapsto \chi + \zeta$, which can be seen as a limit of (15) as $w_0 \to \infty$ and $\beta \to 0$ simultaneously, maintaining $\beta w_0^2 = \zeta$. The orbits of this group are straight lines of the slope $(k_x,\, k_y,\, 0,\, 0)$ in the phase–space, along which the Wolf function is constant. This is at the base of the stability of the solution in terms of phase–space representation and the evolution equation (9). The same argument, however, immediately shows that any solution featuring this symmetry is inevitably unnormalizable because the integral of the Wigner function over the full phase–space involves an integral of a constant over $\mathbb{R}$. For Wolf functions constant in χ we can thus introduce a restricted normalization condition

[4] Up to a factor of 2 this is the effective Hamiltonian of the paraxial wave equation (3).

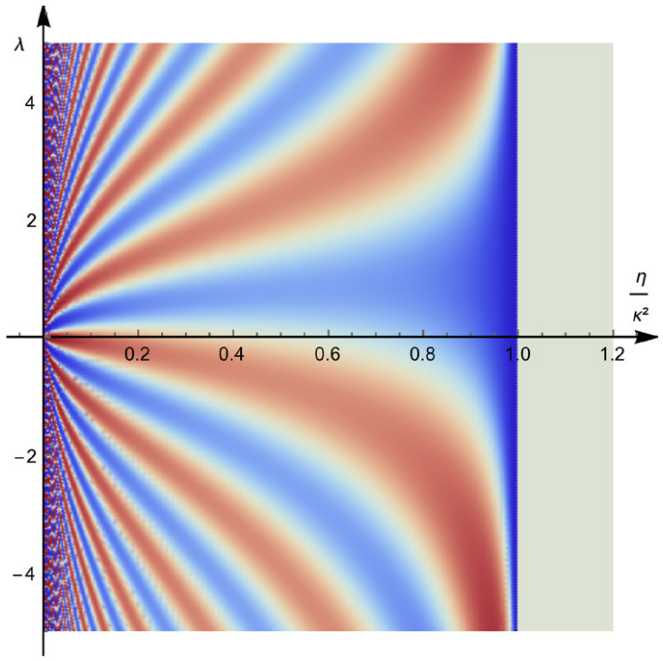

Figure 3. The Wolf function of a Bessel beam with $l = 1$ as a function of η and λ. Each point represents a constant value over a cylinder in phase–space parametrized by θ and χ. The parameter κ only affects the scale of the η axis. There is a discontinuity at $\eta = \kappa^2$: the Wolf function diverges as $O(\eta^{-1/2})$ from the left but is a constant zero for $\eta > \kappa^2$.

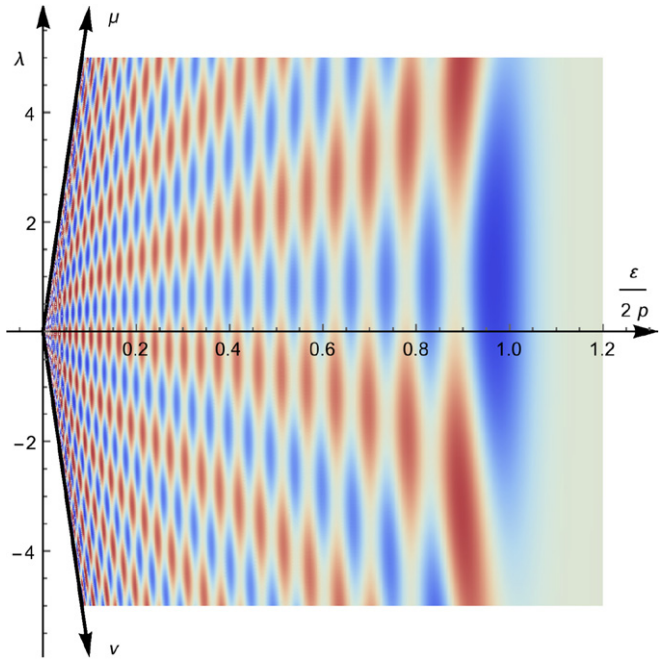

Figure 4. The Wolf function of $LG_{1,30}$ as an approximant to a Bessel beam of $l = 1$ (see figure 3). The horizontal axis was rescaled accordingly to the limit procedure (23). As p further rises, the apparent horizontal ripples get denser but do not decrease in amplitude.

$$\int_0^\infty \mathrm{d}\eta \int_{-\infty}^{\infty} \mathrm{d}\lambda \int_0^{2\pi} \mathrm{d}\theta W(\eta, \lambda, \theta, 0) = 1$$

instead of the full L^1 norm. Note that the prefactors in (22) and (25) were chosen so as to satisfy this condition.

One might naturally expect that the Wolf function (25) could be obtained from (16) using the limit procedure outlined above. We note that this is possible but is analytically challenging as the convergence takes

place in a weak sense only; the latter converges to the former as a distribution but neither pointwise nor in any L-norm. The character of the convergence is illustrated in figure 4.

It follows from the symmetry with respect to (26) that the ray decomposition of a Bessel beam, as described by its Wolf function interpreted as an intensity distribution, will comprise parallel rays of constant intensity arranged in planes defined by the wave vector and the propagation direction. In a cross section, we would observe this as lines of constant flow along their transverse k-vector. The whole space is thus covered by positive and negative rays, non-decreasing in intensity even at high radii but rather asymptotically cancelling each other perfectly. In areas near the beam axis positive rays are more abundant due to the detailed properties of (22), resulting in the characteristic concentric ring intensity profile. All of these aspects can be fully appreciated only at extremely high sample rates, or in motion, as provided by two examples in the Supplementary Material.

Mixtures of Gaussian beams

The preceding examples dealt with individual, perfectly coherent or 'pure' wavefronts. The conditions on purity along with those on rotational symmetry and symmetry with respect to fractional Fourier transform, or to free-space propagation, translate to eigenfunction equations of (11) and (12) or (21) and leave LG or Bessel beams as the only solutions, respectively.

A Wolf function, however, can also be calculated for a statistical mixture of different beams, opening new possibilities for constructing mixed beams exhibiting rotational symmetry and propagational stability. In a sense, the full characterization is trivial: rotational symmetry of a Wolf function alone implies that the field is represented by a single wave function $u(x,\ y)$ which is an eigenfunction of (11) or a statistical mixture thereof; similarly, the symmetry with respect to (15) constrains the individual wave functions composing the field to eigenfunctions of (12) (not necessarily corresponding to the same eigenvalues). If these two conditions are put together, the field is restricted to be a statistical mixture of LG beams with various l and p but of the same beam waist w_0. However, we might still seek for Wolf functions which are special in certain ways.

An interesting class of paraxial field solutions are those which can be written as a statistical mixture of Gaussian beams only. As the Wolf function is linear in the second-order correlation function (represented by the density operator), statistically mixing different components results in an affine combination of their respective Wolf functions, in turn the Wolf functions of any mixture of Gaussian beams is positive in all points. The axial Gaussian beam shows both the required symmetries, as shown above by being a special case of LG_{00}, and we can use it to construct more complicated fields while maintaining both symmetries by forming equal-weight mixtures of its displacements to phase–space points along their phase–space orbits.

The principal case is obtained by displacing the Gaussian Wolf function

$$W_0\left(x,\ y,\ k_x,\ k_y\right) = \frac{1}{\pi^2}\mathrm{e}^{-\left(x^2+y^2\right)/w_0^2-\left(k_x^2+k_y^2\right)w_0^2}$$

along all points $(\tilde{x},\ \tilde{y},\ \tilde{k}_x,\ \tilde{k}_y)$ of constant $\tilde{\mu},\ \tilde{\nu} \in \mathbb{R}$ and integrating with respect to $(1/2\pi)^2\mathrm{d}\tilde{\phi}_1\mathrm{d}\tilde{\phi}_2$:

$$W\left(x,\ y,\ k_x,\ k_y\right) = \frac{1}{4\pi^4}\iint_0^{2\pi}\exp\Bigg(-\Big(\left(x-\tilde{x}\right)^2+\left(y-\tilde{y}\right)^2\Big)\Big/w_0^2-\Big(\left(x_k-\tilde{k}_x\right)^2 + \left(k_y-\tilde{k}_y\right)^2\Big)w_0^2\Bigg)\mathrm{d}\tilde{\phi}_1\mathrm{d}\tilde{\phi}_2,$$

where (see (18))

$$\begin{aligned}
\tilde{x} &= \frac{w_0}{\sqrt{2}}\left(\sqrt{\tilde{\mu}}\cos\tilde{\phi}_1 - \sqrt{\tilde{\nu}}\cos\tilde{\phi}_2\right),\\
\tilde{y} &= \frac{w_0}{\sqrt{2}}\left(\sqrt{\tilde{\mu}}\sin\tilde{\phi}_1 - \sqrt{\tilde{\nu}}\sin\tilde{\phi}_2\right),\\
\tilde{k}_x &= \frac{1}{\sqrt{2}\,w_0}\left(-\sqrt{\tilde{\mu}}\sin\tilde{\phi}_1 - \sqrt{\tilde{\nu}}\sin\tilde{\phi}_2\right),\\
\tilde{k}_y &= \frac{1}{\sqrt{2}\,w_0}\left(\sqrt{\tilde{\mu}}\cos\tilde{\phi}_1 + \sqrt{\tilde{\nu}}\cos\tilde{\phi}_2\right).
\end{aligned}$$

Carrying out the integration and rewriting the results in the coordinates (17), the Wolf function of the mixture is

$$W\left(\mu,\ \nu,\ \phi_1,\ \phi_2\right) = \frac{1}{\pi^2}\mathrm{e}^{-\left(\mu+\nu+\tilde{\mu}+\tilde{\nu}\right)}I_0\left(2\sqrt{\tilde{\mu}\mu}\right)I_0\left(2\sqrt{\tilde{\nu}\nu}\right). \tag{27}$$

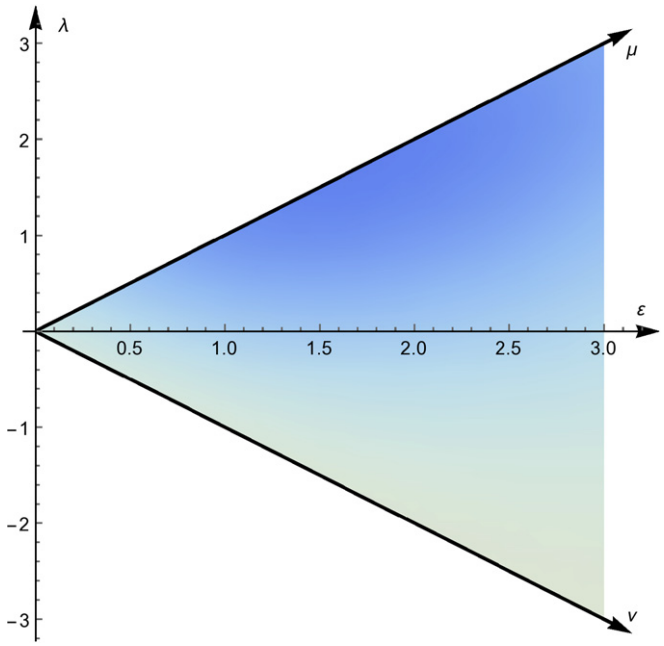

Figure 5. The Wolf function of a statistical mixture of Gaussian beams symmetrized with respect to (14) and (15) in the notation defined in figure 1. The effective $l = 1.5$ and $p = 0.5$ ($\tilde{\mu} = 4$, $\tilde{\nu} = 1$). Note that this Wolf function is never negative.

This corresponds to a mean value of

$$l = \frac{\tilde{\mu} - \tilde{\nu}}{2} \tag{28}$$

and

$$p = \frac{\min\left\{\tilde{\mu}, \tilde{\nu}\right\}}{2}. \tag{29}$$

Clearly, any combination of *real* l and *real* non-negative p can be reached. (It is important that this is not confused with the concept of fractional l values created on spiral waveplates with a non-integer phase step, as described by Beijersbergen *et al* [35] and studied in many later works [36, 37], which are observed in *coherent* superpositions of integer l wavefronts and break the axial symmetry.) An example where l and p are fractional is depicted in figure 5 and a typical cross section of this kind of field in figure 6.

The spatial intensity distribution can be found by integrating $W(x, y, k_x, k_y)$ with respect to k_x and k_y and can be expressed using polar coordinates as an infinite sum of modified Bessel functions,

$$w(r\cos\phi, r\sin\phi) = \frac{1}{\pi w_0^2} \mathrm{e}^{-r^2/w_0^2 - \left(\tilde{\mu}+\tilde{\nu}\right)/2} \sum_{k=-\infty}^{+\infty} I_k\left(\sqrt{2\tilde{\mu}}\frac{r}{w_0}\right) I_k\left(\sqrt{2\tilde{\nu}}\frac{r}{w_0}\right) I_k\left(-\sqrt{\tilde{\mu}\tilde{\nu}}\right). \tag{30}$$

This form does not seem to allow for further analytic simplification. The only exceptions are the cases where $\tilde{\mu} = 0$ or $\tilde{\nu} = 0$. Note that in these cases the beams are mixed only along a circle in phase–space as opposed to a torus for two non-zero variables. If for instance $\tilde{\nu} = 0$, (30) collapses to

$$w(r\cos\phi, r\sin\phi) = \frac{1}{\pi w_0^2} \mathrm{e}^{-r^2/w_0^2 - \tilde{\mu}/2} I_0\left(\sqrt{2\tilde{\mu}}\frac{r}{w_0}\right),$$

the corresponding l value is $\tilde{\mu}/2$ and p is zero. The case $\tilde{\mu} = 0$ is done analogously and describes mixtures with a negative effective angular momentum. Both values at zero correspond to a pure Gaussian beam.

The fields described by (27) can be further statistically mixed, maintaining the non-negativity and symmetry properties but potentially increasing incoherence. In this sense they form the envelope of the convex set of all solutions satisfying the three conditions. For example, upon integration with respect to $\tilde{\mu}$ and $\tilde{\nu}$ with weight factors given by exponential distributions in both parameters, we obtain the Wolf function of the 'twisted Gaussian Schell-model beams' studied earlier by Simon and Mukunda [38], which can be generally expressed in our formalism as

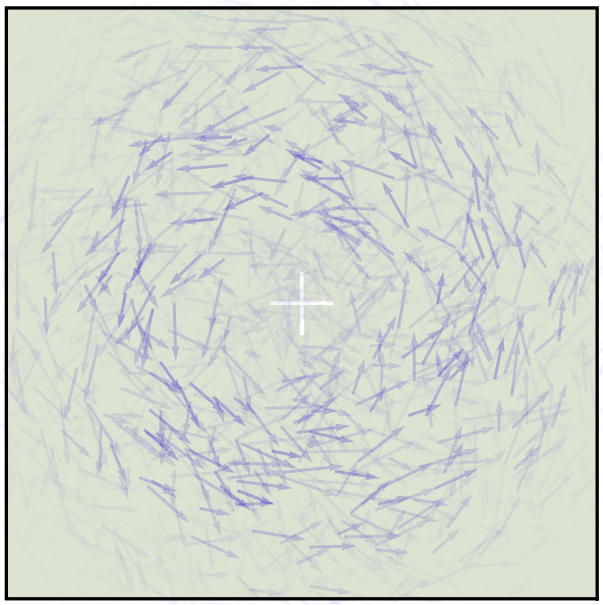

Figure 6. A cross section of a symmetrized mixture of Gaussian beams with $\tilde{\mu} = 3$ and $\tilde{\nu} = 0$, corresponding to $l = 1.5, p = 0$. All other parameters and colour encoding scheme are the same as in figure 2. A similar rotational pattern is clearly visible and no negative rays are necessary in this case.

$$W\left(\mu, \nu, \phi_1, \phi_2\right) = \frac{\alpha\beta}{\pi^2} \mathrm{e}^{-\alpha\mu-\beta\nu}, \quad 0 < \alpha, \beta \leqslant 1 \tag{31}$$

and which also features non-trivial effective l and p numbers, readily obtained as

$$l = \frac{\alpha^{-1} - \beta^{-1}}{2}, \quad p = \frac{\min\left\{\alpha^{-1}, \beta^{-1}\right\} - 1}{2}$$

by either a direct computation using (31) or by averaging (28) and (29) with the same weight distribution.

The mixtures of Gaussian beams described in this section are capable of exerting a torque in a manner similar to LG beams without the presence of helical wave fronts or optical vortices. However, proposed information encoding capabilities of LG beams [10, 12] are hindered by the mutual non-orthogonality of the solutions for different l, p.

The Supplementary Material visualizes the propagation of a generic case of a mixture of Gaussian beams corresponding to $\tilde{\mu} = 2$ and $\tilde{\nu} = 0$ ($l = 1, p = 0$) for a comparison with the corresponding LG mode.

Conclusions

LG and Bessel beams are two important classes of scalar optical beams carrying OAM. They are characterized by rotational symmetry along with preservation of spatial structure under propagation (LG beams) or a full symmetry under free-space propagation (Bessel beams). We presented their respective Wolf functions and how these two symmetries naturally manifest themselves in phase–space. We discussed the role of negativity in the induced generalized ray decomposition and compared our approach to introducing rays as vector lines of the Poynting field.

Furthermore we introduced a simple class of statistical mixtures of Gaussian beams which exhibit similar properties as LG beams: they are rotationally symmetric and preserve the shape of their intensity profile as they propagate along the beam axis. They can be assigned an effective value of non-negative l and p parameters, which are not restricted to integers. More solutions can be obtained by further mixing of these fields.

We know that negativity of the Wigner function is an inevitable effect if non-Gaussian wave functions in quantum mechanics are studied [31], and correspondingly one needs to introduce negative ray pencils in order to describe LG and Bessel beams in terms of generalized ray optics. However our last studied case shows that the negativity of the Wolf function is not a prerequisite for a non-zero l (or p). It only becomes inevitable, along with quantization of the beam parameters, as a consequence of the restriction on 'pure' wavefronts.

Acknowledgments

This work was supported by the EPSRC grant EP/I012451/1, 'Challenges in Orbital Angular Momentum'.

References

[1] Newton I 1952 *Opticks, Or A Treatise of the Reflections, Refractions, Inflections & Colours of Light* (New York: Dover)
[2] Papoulis A 1974 Ambiguity function in Fourier optics *J. Opt. Soc. Am.* **64** 779
[3] Bastiaans M J 1978 The Wigner distribution function applied to optical signals and systems *Opt. Commun.* **25** 26
[4] Bastiaans M J 1978 Transport equations for the Wigner distribution function *Opt. Acta: Int. J. Opt.* **26** 1265
[5] Bastiaans M J 1979 Wigner distribution function and its application to first-order optics *J. Opt. Soc. Am.* **69** 1710
[6] Sudarshan E C G 1979 Pencils of rays in wave optics *Phys. Lett.* A **73** 269
[7] Sudarshan E C G 1980 Geometry of wave electromagnetics *AIP Conf. Proc.* **65** 95
[8] Sudarshan E C G 1986 Three perspectives on light progress *Quantum Field Theory* ed H Ezawa and S Kamefuchi (Amsterdam: North-Holland) pp 325–47 ch 14
[9] Simon R 1983 Generalized pencils of rays in statistical wave optics *Pramāna* **20** 105
[10] Yao A M and Padgett M J 2011 Orbital angular momentum: origins, behavior and applications *Adv. Opt. Photon.* **3** 161
[11] Simpson N B, Allen L and Padgett M J 1996 Optical tweezers and optical spanners with Laguerre–Gaussian modes *J. Mod. Opt.* **43** 2485
[12] Wang J *et al* 2012 Terabit free-space data transmission employing orbital angular momentum multiplexing *Nat. Phot.* **6** 488
[13] Dennis M R and Götte J B 2012 Topological aberration of optical vortex beams: determining dielectric interfaces by optical singularity shifts *Phys. Rev. Lett.* **109** 183903
[14] Heckenberg N R, McDuff R, Smith C P and White A G 1992 Generation of optical phase singularities by computer-generated holograms *Opt. Lett.* **17** 221
[15] Arlt J, Dholakia K, Allen L and Padgett M J 1998 The production of multiringed Laguerre–Gaussian modes by computer-generated holograms *J. Mod. Opt.* **45** 1231
[16] Singh R P, Roychowdhury S and Jaiswal V K 2007 Non-axial nature of an optical vortex and Wigner function *Opt. Commun.* **274** 281–5
[17] Bandyopadhyay A and Singh R P 2011 Wigner distribution of elliptical quantum optical vortex *Opt. Commun.* **284** 256–61
[18] Bandyopadhyay A, Prabhakar S and Singh R P 2011 Entanglement of a quantum optical elliptic vortex *Phys. Lett.* A **375** 1926
[19] Padgett M J and Bowman R 2011 Tweezers with a twist *Nat. Phot.* **5** 343
[20] Ruffner D B and Grier D G 2012 Optical forces and torques in non-uniform beams of light *Phys. Rev. Lett.* **108** 173602
[21] McMorran B J, Agarwal A, Anderson I M, Herzing A A, Lezec H J, McClelland J J and Unguris J 2011 Electron vortex beams with high quanta of orbital angular momentum *Science* **331** 192
[22] Allen L, Beijersbergen M W, Spreeuw R J C and Woerdman J P 1992 Orbital angular momentum of light and the transformation of Laguerre–Gaussian laser modes *Phys. Rev.* A **45** 8185
[23] Allen L and Padgett M J 2000 The Poynting vector in Laguerre–Gaussian beams and the interpretation of their angular momentum density *Opt. Commun.* **184** 67
[24] Berry M V and McDonald K T 2008 Exact and geometrical optics energy trajectories in twisted beams *J. Opt.* A **10** 035005
[25] Leach J, Keen S and Padgett M J 2006 Direct measurement of the skew angle of the Poynting vector in a helically phased beam *Opt. Express* **14** 11919
[26] Barnett S M and Berry M V 2013 Superweak momentum transfer near optical vortices *J. Opt.* **15** 125701
[27] Siegman A E 1986 *Lasers* (Sausalito, CA: University Science Books) pp 276–9
[28] Goodman J W 1996 *Introduction to Fourier Optics* II ed (New York: McGraw-Hill) pp 36–38 61–62
[29] Barnett S M and Radmore P M 1997 *Methods in Theoretical Quantum Optics* (New York: Oxford University Press) pp 106–25
[30] Mandel L and Wolf E 1995 *Optical coherence and quantum optics* (Cambridge, UK: Cambridge University Press) 160–70 p 266
[31] Hudson R L 1974 When is the Wigner quasi-probability density non-negative? *Rep. Math. Phys.* **6** 249
[32] Simon R and Agarwal G S 2000 Wigner representation of Laguerre–Gaussian beams *Opt. Lett.* **25** 1313
[33] Vanvalkenburgh M 2008 Laguerre-Gaussian modes and the Wigner transform *J. Mod. Opt.* **55** 3535
[34] Abramowitz M and Stegun I A (ed) 1972 *Handbook of Mathematical Functions with Formulas Graphs, and Mathematical Tables* (New York: Dover Publications)
[35] Beijersbergen M W, Coerwinkel R P C, Kristensen M and Woerdman J P 1994 Helical-wavefront laser beams produced with a spiral phaseplate *Opt. Commun.* **112** 321–7
[36] Berry M V 2004 Optical vortices evolving from helicoidal integer and fractional phase steps *J. Opt.* A **6** 259–68
[37] Oemrawsingh S S R, Aiello A, Eliel E R, Nienhuis G and Woerdman J P 2004 How to observe high-dimensional two-photon entanglement with only two detectors *Phys. Rev. Lett.* **92** 217901
[38] Simon R and Mukunda N 1993 Twisted Gaussian Schell-model beams *J. Opt. Soc. Am.* A **10** 95–109